

Dimensional resonances in elliptic electron disks

C. Dahl, F. Brinkop, Achim Wixforth, Jörg P. Kotthaus, J.H. English, M. Sundaram

Angaben zur Veröffentlichung / Publication details:

Dahl, C., F. Brinkop, Achim Wixforth, Jörg P. Kotthaus, J.H. English, and M. Sundaram. 1991. "Dimensional resonances in elliptic electron disks." *Solid State Communications* 80 (9): 673–76. [https://doi.org/10.1016/0038-1098\(91\)90885-y](https://doi.org/10.1016/0038-1098(91)90885-y).

DIMENSIONAL RESONANCES IN ELLIPTIC ELECTRON DISKS

C. Dahl, F. Brinkop, A. Wixforth and J. P. Kotthaus
Sektion Physik, Universität München, D-8000 München 22, Germany

J. H. English and M. Sundaram
Materials Dept., University of California, Santa Barbara, CA 93106, USA

We study the anisotropy of the response of a two-dimensional electron gas confined laterally in elliptic geometry at microwave frequencies. In contrast to circular disks the lowest dipole mode is split at zero magnetic field. The resonance positions are quantitatively described by electrons oscillating in a homogeneous depolarization field. We also observe a polarization-dependent higher harmonic of the fundamental low frequency mode.

Dimensional resonances in a two-dimensional electron gas (2DEG) confined to a circular disk have been intensively investigated since their first observation by Allen et al.¹. Small disks containing only few electrons, the so-called quantum dots have been studied in InSb- and Si-MOS structures^{2,3} as well as in GaAs-heterostructures^{4,5}. Comparatively macroscopic systems have been studied in GaAs-heterostructures with diameters ranging from about $d=50\mu\text{m}$ ^{6,7} up to several mm^{8,9}. The same type of resonances has also been observed in the electron layer electrostatically induced on the surface of liquid helium^{10,11}. The high frequency response of such disks can be understood in classical terms as originally formulated by Maxwell-Garnett¹². Basically, the carriers oscillate in the depolarization field arising from a displacement from their equilibrium positions by an external perturbation. In the dipole approximation this is equivalent to the independent motion of electrons in a harmonic potential. The resonance positions are then given by

$$\omega_{\pm} = \pm\omega_c/2 + (\omega_c^2/4 + \omega_0^2)^{1/2} \quad (1)$$

where ω_0 is the plasma frequency at zero magnetic field, or, equivalently, $m^*\omega_0^2$ the curvature of the external potential. Eq.(1) equally applies to quantum dots provided the external potential is harmonic^{13,14}. In a finite magnetic field B the resonance splits into two modes which are qualitatively different at large B . The high frequency mode approaches the cyclotron resonance frequency, independent of the geometry, whereas the low frequency mode decreases as $1/(Bd)$, independent of the effective mass. The lower mode is driven by the Hall current perpendicular to the depolarization field which in effect leads to a rotation of the internal fields and currents^{15,16} with the frequency ω_- . In an anharmonic potential or in inhomoge-

neous external fields higher harmonics of the fundamental mode (1) can also be excited as has been observed in large electron discs on the surface of liquid helium¹¹.

If the symmetry of the system is reduced, the degeneracy of the resonance (1) at zero magnetic field is lifted. This behavior is demonstrated here for a rectangular array of elliptic 2D disks in a MBE-grown, modulation-doped GaAs/AlGaAs-heterostructure. The Si-doping region in the heterostructure is set back from the GaAs/AlGaAs-interface by a 20 nm spacer. The dimensions of the ellipses are $116\mu\text{m}$ for the major and $40\mu\text{m}$ for the minor axis, and their periodicity along these axes is 165 and $70\mu\text{m}$, respectively. The lateral structure is defined by standard contact lithography and wet mesa etching. Before processing, the sample had an electron concentration of $n_s = 3 \cdot 10^{11} \text{ cm}^{-2}$ and a mobility of $\mu = 5 \cdot 10^5 \text{ cm}^2/\text{Vs}$ at $T=4.2\text{K}$ in the dark. The resonances are studied in the millimeter wave regime from 24 to 230 GHz using a scalar network analyzer (AB Millimetre). The sample is placed into a Ka-band waveguide in the center of a superconducting solenoid at liquid helium temperature. We measure the transmitted microwave power as function of the magnetic field at fixed frequency in the dark.

Typical spectra are shown in Fig.1 for polarization along the major ("parallel polarization", Fig.1a) and minor axis ("perpendicular polarization", Fig.1b), respectively. From 24 to ~55 GHz the resonance positions shift to lower magnetic fields with increasing frequency. Between 70 and 130 GHz an additional resonance is observed in parallel polarization which also shifts to lower fields with increasing frequency. In perpendicular polarization no resonances can be identified in this frequency regime and only a Drude-like decrease of absorption is seen in the transmitted signal. Above ~135 GHz the resonance positions shift to higher fields with increasing frequency.

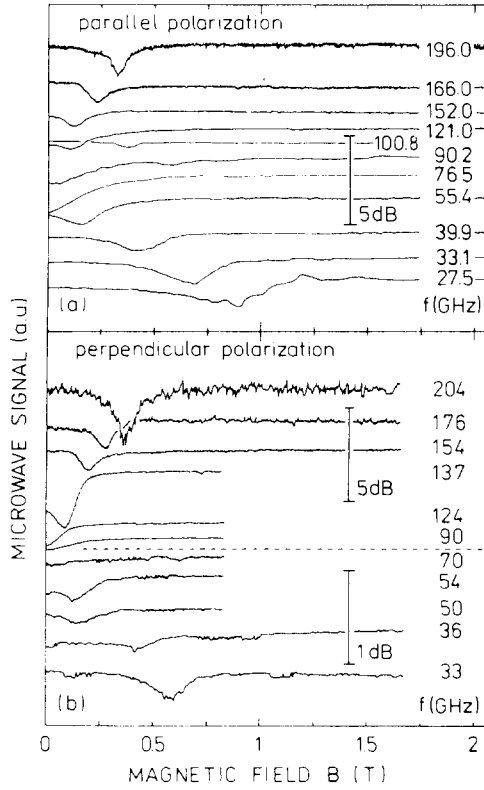


Fig.1. Transmitted millimeter wave signal versus the magnetic field of $116 \times 40 \mu\text{m}$ electron ellipses at $T=2\text{K}$ for a) parallel polarization (millimeter wave polarized along the major axis), $n_s = 3.4 \times 10^{11} \text{ cm}^{-2}$,

b) perpendicular polarization (millimeter wave polarized along the minor axis), $n_s = 2.8 \times 10^{11} \text{ cm}^{-2}$.

The traces are offset for clarity. The different densities n_s in (a) and (b) are a consequence of two different cool-down cycles. Note the different scales in the upper and lower part of (b).

To explain the resonance positions quantitatively, we model the 2D electron ellipses as thin 3D ellipsoids with thickness $2c$ and semimajor and semiminor axes a and b and neglect electrostatic coupling between different ellipses. In such a system the effective conductivity tensor is readily obtained by solving the classical equations of motion:

$$\sigma_{\text{eff}} = \frac{i\omega n_s e^2 / m^*}{(\omega^2 - \omega_x^2 + i\omega/\tau)(\omega^2 - \omega_y^2 + i\omega/\tau) - \omega^2 \omega_c^2} \times \begin{pmatrix} \omega^2 - \omega_y^2 + i\omega/\tau & -i\omega\omega_c \\ i\omega\omega_c & \omega^2 - \omega_x^2 + i\omega/\tau \end{pmatrix} \quad (2)$$

The quantities

$$\begin{aligned} \omega_x^2 &= \omega_p^2 L_x \\ \omega_y^2 &= \omega_p^2 L_y \end{aligned} \quad (3)$$

are the plasma frequencies of the ellipsoid at $B=0$ for polarization parallel and perpendicular to the major axis, respectively. In eq.(3) ω_p is the plasma frequency of the homogeneous 3D electron gas. The effective conductivity tensor relates the current to the external field rather than to the total field $\mathbf{E} = \mathbf{E}_{\text{ext}} - \mathbf{LP}$ and hence describes the power absorbed from the applied millimeter wave field. The components of the (diagonal) depolarization tensor¹⁷ L

$$\begin{aligned} L_x &= \frac{cb}{a^2} \frac{K(\eta) - E(\eta)}{\eta^2} \\ L_y &= \frac{c}{b} \frac{E(\eta) - (1 - \eta^2)K(\eta)}{\eta^2} \end{aligned} \quad (4)$$

represent the influence of the geometry on the depolarization field and thus the restoring force when the mobile carriers are displaced by the external field with respect to the background charge. Here, K and E are complete elliptic integrals and $\eta^2 = 1 - b^2/a^2$ is the eccentricity of the ellipse. For $c \ll b$ one can introduce the sheet density via $n_s = nV/A$ where V is the volume and A the projected area of the ellipsoid so that

$$\begin{aligned} \omega_x^2 &= \frac{3n_s e^2 b}{4\epsilon\epsilon_0 m^* a^2} \frac{K(\eta) - E(\eta)}{\eta^2} \\ \omega_y^2 &= \frac{3n_s e^2}{4\epsilon\epsilon_0 m^* b} \frac{E(\eta) - (1 - \eta^2)K(\eta)}{\eta^2} \end{aligned} \quad (5)$$

From (2) we obtain the resonance positions (for $\omega\tau \gg 1$) as function of the magnetic field:

$$\omega_{\pm}^2 = (\omega_x^2 + \omega_y^2 + \omega_c^2)/2 \pm \{(\omega_x^2 + \omega_y^2 + \omega_c^2)^2/4 - \omega_x^2 \omega_y^2\}^{1/2}. \quad (6)$$

In Fig.2 we compare experimentally observed frequencies in their dependence on the magnetic field with calculated ones for both polarizations. For the case of parallel polarization the best fit to the resonance positions according to eq.(6) is obtained with $\omega_x/2\pi = 63 \text{ GHz}$ and $\omega_y/2\pi = 140 \text{ GHz}$ using an appropriate effective mass of $m^* = 0.069m_e$. With the experimentally determined density $n_s = 3.4 \times 10^{11} \text{ cm}^{-2}$ and the dielectric constant for the half space, $\epsilon = (\epsilon_{\text{GaAs}} + 1)/2 = 6.8$, eq. (5) yields $\omega_x/2\pi = 64 \text{ GHz}$ and $\omega_y/2\pi = 143 \text{ GHz}$ well consistent with the above values. The density is obtained from Shubnikov-de Haas oscillations visible in the microwave signal for lower frequencies at $T=2\text{K}$. Thermal cycling of the sample between the two different polarization measurements is the origin of the somewhat lower density $n_s = 2.8 \times 10^{11} \text{ cm}^{-2}$ that is ob-

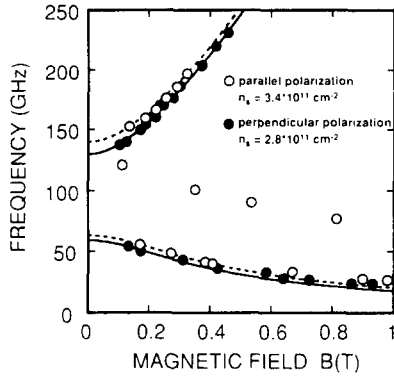


Fig.2. Resonance positions of the traces displayed in Fig.1. The lines are fits according to eq.(6), for the parallel (---) and perpendicular (—) geometry, respectively, with fit parameters given in the text.

tained for the measurements in perpendicular polarization. This results in lower plasma frequencies $\omega_x/2\pi=59$ GHz and $\omega_y/2\pi=130$ GHz, values that are both in good agreement with eq.(5).

At zero magnetic field only the mode with the same polarization as the incident radiation is excited. This is different in a finite magnetic field, since the modes are no longer linearly polarized. The oscillator strength of the individual modes, however, still depends on the polarization. This can be seen in the transmission traces of Fig.1, particularly for the lower mode. For polarization along the major axis the signal of the lower mode is considerably stronger than for polarization along the minor axis.

For the low frequency branch the resonance positions at higher magnetic fields are seen to be higher than eq.(6) suggests. This feature has been observed for circular disks before⁶ and reveals the limits of the ellipsoidal model, whose main disadvantage is the implicit assumption of a nonuniform sheet density.

As mentioned above a further resonance appears in parallel polarization. We interpret this mode as a higher harmonic with respect to the "radial" mode index. Modes with higher azimuthal index are not excited in an external dipole field. Similar excitations have been observed in circular electron discs on the surface of liquid helium¹¹. In the elliptic system this mode is also no longer degenerate at $B=0$, and we here observe its low frequency branch which (at $B=0$) is also polarized along the major axis. At finite magnetic fields this resonance should in principle be observable in the "wrong" polarization as well, but is presumably too weak to be seen here. Hence for perpendicular polarization the signal only exhibits a Drude-like tail in the frequency regime between $\omega_x/2\pi$ and $\omega_y/2\pi$. The magnetic field dependence of the harmonic mode is, however,

different from the analogous circular mode. Presently, we have no quantitative theory of such modes in the elliptic case. However, we expect the upper branch of this higher harmonic to be well above $\omega_y/2\pi$ and therefore not accessible to our present experimental setup. At high magnetic fields the response of the system should be isotropic with $\omega_- \approx \omega_x \omega_y / \omega_c$ and $\omega_+ \approx \omega_c$ to leading order in ω_c , i.e. the ellipse then behaves equivalently to a circular disk with plasma frequency $\omega_0 = (\omega_x \omega_y)^{1/2}$.

In conclusion we have observed plasma resonances of elliptic 2D electron disks in the millimeter wave regime. In contrast to geometries with fourfold symmetry the lowest dipole modes are no longer degenerate at zero magnetic field. Their values agree well with the classical Maxwell-Garnett theory¹² with the system modelled as uncoupled thin 3D ellipsoids. This indicates that electrostatic coupling of the elliptic disks is not important here. At higher magnetic fields the resonance positions of the low frequency mode deviate from the ellipsoidal model. Here a truly 2D calculation would be more appropriate. The anisotropy of the response is seen as a dependence of the signal strength of the low frequency mode on the polarization. Above the fundamental low frequency mode the system shows a second branch of polarization-dependent resonances which shift to lower magnetic fields with increasing frequency. In analogy to the spectrum observed in circular disks we believe this mode to be a higher harmonic with respect to the radial mode index, generalized to the elliptic geometry.

Acknowledgement - We gratefully acknowledge financial support by the Deutsche Forschungsgemeinschaft and the ESPRIT Basic Research Action.

References

1. S.J. Allen, Jr., H.L. Störmer, and J.C.M. Hwang, Phys. Rev. B **28**, 4875 (1983)
2. Ch. Sikorski and U. Merkt, Phys. Rev. Lett. **62**, 2164 (1989)
3. J. Alsmeier, E. Batke and J.P. Kotthaus, Phys. Rev. B **41**, 1699 (1990)
4. A. Lorke, J.P. Kotthaus, and K. Ploog, Phys. Rev. Lett. **64**, 2559 (1990)
5. T. Demel, D. Heitmann, P. Grambow, and K. Ploog, Phys. Rev. Lett. **64**, 788 (1990)
6. F. Brinkop, C. Dahl, J.P. Kotthaus, G. Weimann, and W. Schlapp, in *High Magnetic Fields in Semiconductor Physics III*, edited by G. Landwehr (Springer, Heidelberg, 1991)
7. L.A. Galchenkov, I.M. Grodnenskii, M.V. Kostovetskii, O.R. Matov, B.A. Medvedev, and V.G. Mokerov, Fiz. Tekh. Poluprovodn. **22**, 1196 (1988) [Sov. Phys. Semicond. **22**, 757 (1988)]
8. M. Wassermeier, J. Oshinowo, J.P. Kotthaus, A.H. MacDonald, C.T. Foxon, and J.J. Harris, Phys. Rev. B **41**, 10287 (1990)

- ⁹I.M. Grodnenskii and A.Yu. Kamaev, *Surf. Sci.* **229**, 522 (1990)
- ¹⁰D.B. Mast, A.J. Dahm, and A.L. Fetter, *Phys. Rev. Lett.* **54**, 1706 (1985)
- ¹¹D.C. Glatli, E.Y. Andrei, G. Deville, J. Poitrenaud, and F.I.B. Williams, *Phys. Rev. Lett.* **54**, 1710 (1985)
- ¹²J.C. Maxwell-Garnett, *Philos. Trans. R. Soc. London* **203**, 385 (1904)
- ¹³L. Brey, N.F. Johnson, and B.I. Halperin, *Phys. Rev. B* **40**, 10647 (1989)
- ¹⁴P.A. Maksym, and T. Chakraborty, *Phys. Rev. Lett.* **65**, 108 (1990)
- ¹⁵V. Talyanskii, *Zh. Eksp. Teor. Fiz.* **92**, 1845 (1987) [*Sov. Phys. JETP* **65**, 6036 (1987)]
- ¹⁶V.A. Volkov and S.A. Mikhailov, *Zh. Eksp. Teor. Fiz.* **94**, 217 (1988) [*Sov. Phys. JETP* **67**, 1639 (1988)]
- ¹⁷J.A. Osborn, *Phys. Rev.* **67**, 351 (1945)